

## Origins of Cell Selectivity of Cationic Steroid Antibiotics

Bangwei Ding, Ning Yin, Yang Liu, Jaime Cardenas-Garcia, Richard Evanson,  
Thomas Orsak, Mingjin Fan, Gracija Turin, and Paul B. Savage\*Contribution from the Department of Chemistry and Biochemistry, Brigham Young University,  
Provo, Utah 84602

Received May 25, 2004; E-mail: paul\_savage @byu.edu

**Abstract:** A key factor in the potential clinical utility of membrane-active antibiotics is their cell selectivity (i.e., prokaryote over eukaryote). Cationic steroid antibiotics were developed to mimic the lipid A binding character of polymyxin B and are shown to bind lipid A derivatives with affinity greater than that of polymyxin B. The outer membranes of Gram-negative bacteria are comprised primarily of lipid A, and a fluorophore-appended cationic steroid antibiotic displays very high selectivity for Gram-negative bacterial membranes over Gram-positive bacteria and eukaryotic cell membranes. This cell selectivity of cationic steroid antibiotics may be due, in part, to the affinity of these compounds for lipid A.

## Introduction

Bacterial membranes are increasingly recognized as effective targets for the development of antibacterial agents. Organisms ranging from bacteria to mammals produce antibiotics that target bacterial membranes,<sup>1</sup> and many new antibiotics have been designed to mimic the actions of endogenous peptide antibiotics. These designed antibiotics have been prepared from  $\alpha$ -amino acids,<sup>2</sup>  $\beta$ -amino acids,<sup>3</sup> arylamide oligomers,<sup>4</sup> peptoids,<sup>5</sup> and amphiphilic steroids.<sup>6,7</sup> A common feature of these antibiotics is that they present or adopt cationic, facially amphiphilic structures or substructures. This morphology allows them to disrupt bacterial membranes at relatively low concentrations.<sup>1–7</sup> While many naturally occurring peptide antibiotics target gross

bacterial membrane structure rather than individual components of the membrane,<sup>8</sup> some peptide antibiotics target specific bacterial membrane features. For example, nisin displays high affinity for lipid II in bacterial membranes, and the antibacterial activity of nisin is much greater than that of other peptide antibiotics.<sup>9</sup> Similarly, polymyxin B has been characterized as selectively binding lipid A,<sup>10–12</sup> the primary constituent of the outer membranes of Gram-negative bacteria, and this peptide antibiotic is highly active against most strains of bacteria producing lipid A.

Interactions of lipid A and polymyxin B have been the subject of a number of studies designed to determine the roles of noncovalent interactions in association.<sup>10–12</sup> These studies have involved use of lipid A isolated from bacteria as well as synthetic versions of lipid A, and tools used in studying lipid A–polymyxin B complexes include NMR<sup>10</sup> and fluorescence spectroscopy<sup>11</sup> and titration calorimetry.<sup>12</sup> In models of lipid A association with polymyxin B, ionic interactions play a central role. For example, Suroliia and co-workers<sup>11</sup> proposed a two-step association process in which ionic interactions cause initial complex formation, and from NMR and corresponding calculated structures Jain and co-workers<sup>10</sup> proposed a compelling model of complex formation involving ionic interactions

- (1) Over 500 naturally occurring antibacterial peptides have been characterized. For leading reviews see: (a) Hancock, R. E. W.; Scott, M. G. *Proc. Natl. Acad. Sci. U.S.A.* **2000**, *97*, 8856–8861. (b) Van't Hof, W.; Veerman, E. C. I.; Helmerhorst, E. J.; Amerongen, A. V. N. *Biol. Chem.* **2001**, *382*, 597–619. (c) Yang, D.; Biragyn, A.; Hoover, D. M.; Lubkowsky, J.; Oppenheim, J. J. *Annu. Rev. Immunol.* **2004**, *22*, 181–215.
- (2) For examples see: (a) Muhle, S.; Tam, J. P. *Biochemistry* **2001**, *40*, 5777–5785. (b) McInnes, C.; Kondejewski, L. H.; Hodges, R. S.; Sykes, B. D. *J. Biol. Chem.* **2000**, *275*, 14287–14294. (c) Schwab, U.; Gilligan, P.; Jaynes, J.; Henke, D. *Antimicrob. Agents Chemother.* **1999**, *43*, 1435–1440.
- (3) (a) Porter, E. A.; Weisblum, B.; Gellman, S. H. *J. Am. Chem. Soc.* **2002**, *124*, 7324–7330. (b) Liu, D.; DeGrado, W. F. *J. Am. Chem. Soc.* **2001**, *123*, 7553–7559. (c) Porter, E. A.; Wang, X.; Lee, H.-S.; Weisblum, B.; Gellman, S. H. *Nature* **2000**, *404*, 565.
- (4) Liu, D.; Choi, S.; Chen, B.; Doerksen, R. J.; Clements, D. J.; Winkler, J. D.; Klein, M. L.; DeGrado, W. F. *Angew. Chem., Int. Ed.* **2004**, *43*, 1158–1162.
- (5) Patch, J. E.; Barron, A. E. *J. Am. Chem. Soc.* **2003**, *125*, 12092–12093.
- (6) (a) Li, C.; Peters, A. S.; Meredith, E. L.; Allman, G. W.; Savage, P. B. *J. Am. Chem. Soc.* **1998**, *120*, 2961–2962. (b) Rehman, A.; Li, C.; Budge, L. P.; Street, S. E.; Savage, P. B. *Tetrahedron Lett.* **1999**, *40*, 1865–1869. (c) Li, C.; Lewis, M. R.; Gilbert, A. B.; Noel, M. D.; Scoville, D. H.; Allman, G. W.; Savage, P. B. *Antimicrob. Agents Chemother.* **1999**, *43*, 1347–1349. (d) Li, C.; Budge, L. P.; Driscoll, C. D.; Willardson, B. M.; Allman, G. W.; Savage, P. B. *J. Am. Chem. Soc.* **1999**, *121*, 931–940. (e) Zhou, X.-T.; Rehman, A.; Li, C.; Savage, P. B. *Org. Lett.* **2000**, *2*, 3015–3018. (f) Guan, Q.; Schmidt, E. J.; Boswell, S. R.; Li, C.; Allman, G. W.; Savage, P. B. *Org. Lett.* **2000**, *2*, 2837–2840. (g) Schmidt, E. J.; Boswell, S. R.; Walsh, J. P.; Schellenberg, M. M.; Winter, T. W.; Li, C.; Allman, G. W.; Savage, P. B. *J. Antimicrob. Chemother.* **2001**, *47*, 671–674. (h) Ding, B.; Guan, Q.; Walsh, J. P.; Boswell, J. S.; Winter, T. W.; Winter, E. S.; Boyd, S. S.; Li, C.; Savage, P. B. *J. Med. Chem.* **2002**, *45*, 663–669.
- (7) Kikuchi, K.; Bernard, E. M.; Sadownik, A.; Regen, S. L.; Armstrong, D. *Antimicrob. Agents Chemother.* **1997**, *41*, 1433–1438.

- (8) Enantiomers of naturally occurring peptide antibiotics have the same antibacterial activity as the parent antibiotics: Wade, D.; Boman, A.; Wählin, B.; Drain, C. M.; Andreu, D.; Boman, H. G.; Merrifield, R. B. *Proc. Natl. Acad. Sci. U.S.A.* **1990**, *87*, 4761–4765.
- (9) (a) Breukink, E.; Wiedemann, I.; van Kraaij, C.; Kuipers, O. P.; Sahl, H.-G.; de Kruijff, B. *Science* **1999**, *286*, 2361–2364. (b) Wiedemann, I.; Breukink, E.; Van Kraaij, C.; Kuipers, O. P.; Bierbaum, G.; De Kruijff, B.; Sahl, H.-G. *J. Biol. Chem.* **2001**, *276*, 1772–1779.
- (10) Bruch, M. D.; Cajal, Y.; Koh, J. T.; Jain, M. K. *J. Am. Chem. Soc.* **1999**, *11993*–12004.
- (11) Thomas, C. J.; Gangadhar, B. P.; Suroliia, N.; Suroliia, A. *J. Am. Chem. Soc.* **1998**, *120*, 12428–12434.
- (12) (a) Srimal, S.; Suroliia, N.; Balasubramanian, S.; Suroliia, A. *Biochem. J.* **1996**, *315*, 679–686. (b) Koch, P.-J.; Frank, J.; Schüler, J.; Kahle, C.; Bradeczek, H. *J. Colloid Interface Sci.* **1999**, *213*, 557–564. (c) Brandenburg, K.; Moriyon, I.; Arraiza, M. D.; Lewark-Yvetot, G.; Koch, M. H. J.; Seydel, U. *Thermochim. Acta* **2002**, *382*, 189–198. (c) Ning, Y.; Marshall, R. L.; Matheson, S.; Savage, P. B. *J. Am. Chem. Soc.* **2003**, *125*, 2426–2435.

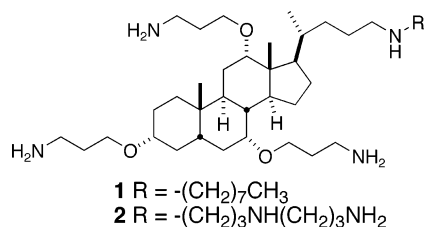


**Figure 1.** Structures of cationic steroid antibiotics **1** and **2**.

between the phosphates on lipid A and the amine groups on polymyxin B.

A class of cationic steroid antibiotics was developed with the intent of mimicking the antibacterial activities of polymyxin B.<sup>6</sup> These antibiotics display antibacterial activity comparable or superior to that of polymyxin B against Gram-negative bacteria,<sup>6c</sup> and examples of the steroid antibiotics effectively permeabilize the outer membranes of Gram-negative bacteria,<sup>6a,c,d</sup> a behavior of a polymyxin derivative attributed to lipid A binding.<sup>13</sup> These observations suggest that cationic steroid antibiotics may bind lipid A with affinities similar to that of polymyxin B. To compare cationic steroid antibiotic and polymyxin B affinities for lipid A, we measured the association of these antibiotics with a lipid A derivative that has been used to characterize the association of polymyxin B with lipid A.<sup>12d</sup>

A central issue in the potential development of membrane-targeting compounds into clinically useful antibiotics is cell selectivity.<sup>1c,14</sup> To the extent that membrane-targeting antibiotics associate with bacterial cells and leave host cells unharmed, they may find unrestricted use in treating infection. Endogenous peptide antibiotics as well as designed membrane-targeting antibiotics exhibit a spectrum of cell selectivities<sup>1–7</sup> as measured indirectly by comparison of antibacterial activities versus hemolytic properties (disruption of red blood cells). In the case of cationic steroid antibiotics, for example, **1** (Figure 1) has a minimum inhibition concentration (MIC) with *Pseudomonas aeruginosa* of 2.0  $\mu\text{g}/\text{mL}$  and a minimum hemolytic concentration (MHC) of 29  $\mu\text{g}/\text{mL}$ ,<sup>6d</sup> while **2** (Figure 1) retains antibacterial activity yet has an MHC of >200  $\mu\text{g}/\text{mL}$ .<sup>6h</sup> Considering that examples of cationic steroid antibiotics appear to bind lipid A and that indirect measurements of cell selectivity suggest that these antibiotics discriminate among cell types, we developed a means of directly observing cell selectivities with fluorophore-appended antibiotics using intact prokaryotic and eukaryotic cells to observe if the affinity of steroid antibiotics for lipid A correlates with cell selectivity.

## Results and Discussion

For studies with lipid A derivatives, we elected to use **3** (Figure 2) because we had been able to characterize its binding with polymyxin B earlier, and we were able to synthesize it in sufficient quantities for use in our titrations.<sup>12d</sup> This derivative presents the intact disaccharide structure of lipid A; deviations from lipid A are in the acyl chains. These deviations allow study with monomeric forms of the glycolipid, and measurements were made at concentrations well below the critical aggregation concentration of **3** (ca. 20  $\mu\text{M}$ ).

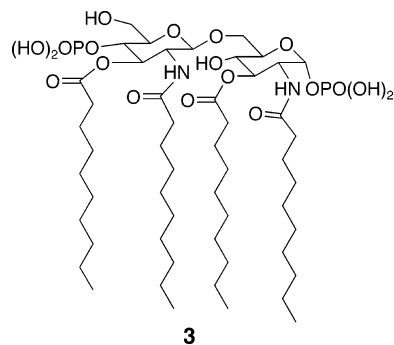


**Figure 2.** Structure of lipid A derivative **3**.

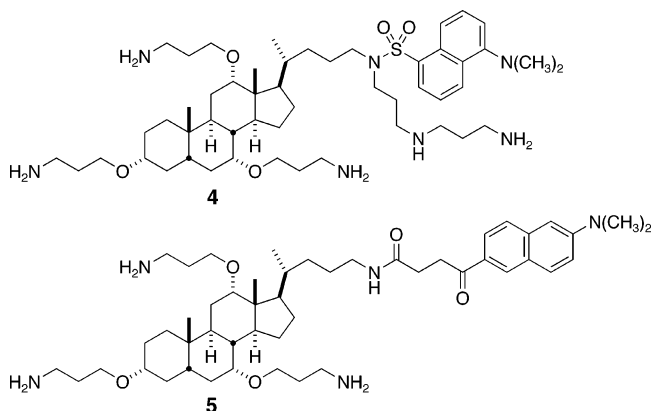


**Figure 3.** Structures of fluorophore-appended cationic steroid antibiotics **4** and **5**.

To observe binding and cell selectivities, we used modulation of fluorescence of small fluorophores appended on cationic steroid antibiotics. Dansyl and prodan groups are known to respond to the polarity of their environments via shifts in fluorescence emission wavelengths and changes in fluorescence intensity.<sup>15,16</sup> We anticipated that fluorophore-appended cationic steroid antibiotics (e.g., **4** and **5** in Figure 3) would display modulations in emission concomitant with association with lipid A and whole bacteria. For measurement of association with **3**, a dansyl fluorophore was used, and to enhance solubility, a diamine chain was appended to the dansyl-labeled antibiotic, giving compound **4**. For measurement of cell selectivities, we expected to be able to observe very small numbers of bacteria with very low concentrations of the fluorophore-labeled antibiotic. Consequently, we elected to use a prodan derivative for these experiments, giving compound **5** (Figure 3), due to the better fluorescent response of this fluorophore as compared to a dansyl group. Also, a key requirement for this labeled compound was that it could be used well below its MIC value so that we could be assured that we were observing interactions with intact bacteria. To keep the MIC value relatively high, we did not add the diamine chain found in **4**.

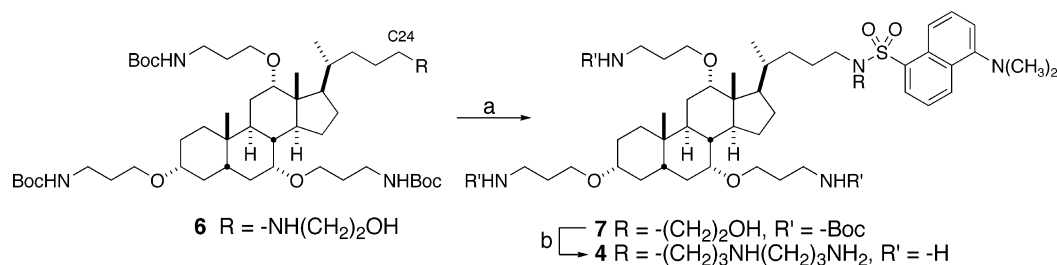
To prepare dansyl-labeled compound **4**, we began with **6** (Scheme 1),<sup>6h</sup> which was coupled with dansyl chloride, giving **7**. Mesylation of the resulting alcohol was followed by addition of *N*-Boc-1,3-diaminopropane. Deprotection of the Boc groups gave **4** as its hydrochloride salt. Compound **8**, used in the preparation of **5** (Scheme 2), is a Boc-protected form of a cationic steroid antibiotic previously reported.<sup>6d</sup> The hydroxyl

(13) Vaara, M.; Viljanen, P. *Antimicrob. Agents Chemother.* **1985**, *27*, 548–554.

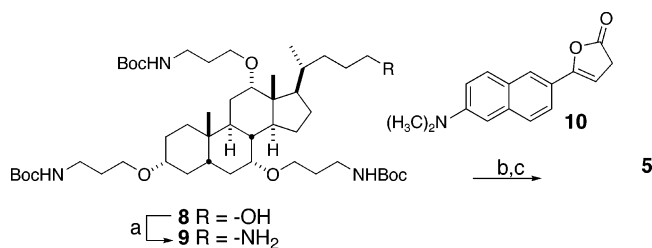
(14) Hancock, R. E. W. *Exp. Opin. Invest. Drugs* **2001**, *9*, 1723–1729.

(15) For example, see: Herron, J. N.; Voss, E. W. *J. Biochem. Biophys. Methods* **1981**, *5*, 1–17.

(16) Weber, G.; Farris, F. J. *Biochemistry* **1979**, *18*, 3075–3078.

**Scheme 1.** Preparation of Fluorophore-Labeled Cationic Steroid Antibiotic **4**<sup>a</sup>

<sup>a</sup> Reagents (yields in parentheses): (a) dansyl chloride, Et<sub>3</sub>N, CH<sub>2</sub>Cl<sub>2</sub> (91%); (b) MsCl, Et<sub>3</sub>N, CH<sub>2</sub>Cl<sub>2</sub>; *N*-Boc-1,3-propyldiamine, Na<sub>2</sub>CO<sub>3</sub>, NaI, THF; 4 M HCl in dioxane (50% overall).

**Scheme 2.** Preparation of Fluorophore-Labeled Cationic Steroid Antibiotic **5**<sup>a</sup>

<sup>a</sup> Reagents (yields in parentheses): (a) MsCl, Et<sub>3</sub>N, CH<sub>2</sub>Cl<sub>2</sub>; NaN<sub>3</sub>, DMSO, THF; Ph<sub>3</sub>P, H<sub>2</sub>O, THF (77% overall); (b) **10**, CH<sub>2</sub>Cl<sub>2</sub> (85%); (c) 4 M HCl in dioxane (100%).

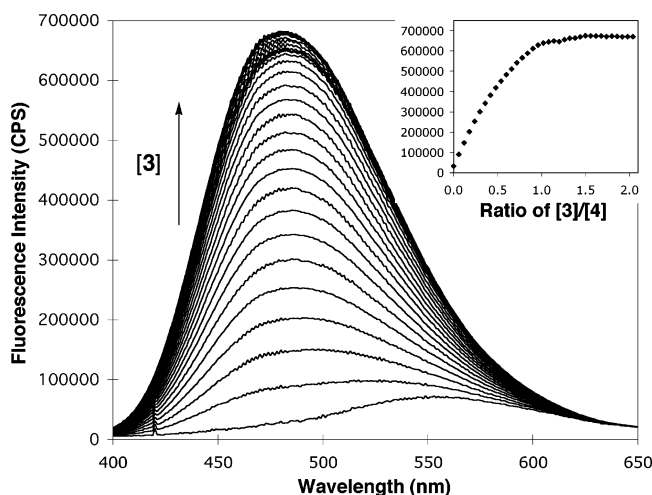


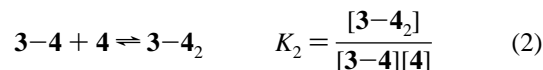
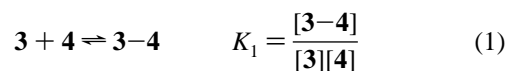
**Figure 4.** Fluorescent spectra from a titration of **4** with **3**. Titration was done in aqueous phosphate buffer (5 mM) at pH 7.2. The initial concentration of **4** was 5  $\mu\text{M}$ . Inset: fluorescence intensity (CPS) at 490 nm vs the ratio of **3** and **4**.

group at C24 was replaced by an amine, which was then reacted with prodan derivative **10**. We recently reported the synthesis of the succinimidyl ester of 4-(6-dimethylaminonaphthalen-2-yl)-4-oxobutyric acid,<sup>17</sup> and we have found that upon extended reaction times it converts to **10**. Compound **10** readily reacts with primary and secondary amines to form the corresponding amides in good yields with the formation of no byproducts. Following reaction of **9** with **10**, removal of the Boc protecting groups yielded **5** as its hydrochloride salt.

Titration of **3** into a phosphate-buffered solution of **4** resulted in a pronounced shift in the emission wavelength of **4** with a large increase in fluorescence intensity (results from a representative titration are shown in Figure 4). This increase reached a maximum at a ratio of **3** to **4** of ca. 1, and further addition of **3** did not result in significant changes in fluorescence emission.

To verify that the relationship of the changes in fluorescence were not due to changes in aggregation state, we performed the titration at lower concentrations of binding partners and observed the same result (i.e., maximum fluorescence modulation at a ratio of **3** to **4** of ca. 1).

Modeling of titration data for interactions of **3** with **4**<sup>18</sup> gave an association constant of  $(1.70 \pm 0.16) \times 10^6 \text{ M}^{-1}$  for 1:1 complex formation and suggested that a weaker 1:2 (**3**:**4**) complex forms with an association constant of  $(3.5 \pm 1.0) \times 10^5 \text{ M}^{-1}$ . Association constants for formation of 1:2 complexes can be represented in stepwise fashion as shown in eqs 1 and 2, with  $K_1$  and  $K_2$  representing the equilibrium constants.



Because polymyxin B is often viewed as the paradigm of lipid A binding by small molecules, we directly compared the affinity of polymyxin B for lipid A to that of **4**. The association of polymyxin B with lipid A in bacterial membranes has been observed via fluorescence modulation using fluorophore-appended polymyxin B.<sup>11a,19</sup> However, polymyxin B presents multiple amine groups, and in the reported work it was not clear where polymyxin B was appended. In addition, it is not clear how substitution at the various amine groups in polymyxin B influences association with lipid A. In contrast, the simplicity of the syntheses of cationic steroid antibiotics facilitates site-specific functionalization. Consequently, rather than attempt to functionalize polymyxin B, we used a displacement assay to compare the affinities of **4** and polymyxin B for **3**.

Titration of the **3-4** complex with polymyxin B resulted in a decrease in the fluorescence intensity of the appended dansyl group (a representative titration is shown in Figure 5A), suggesting that polymyxin B displaces **4** from **3**. A cursory examination of these titration data indicates that much more than 1 equiv of polymyxin B is required to displace **4** from **3**. This result suggests that **4** has higher affinity for **3** than polymyxin B. Mathematical modeling of the exchange reaction is complicated by the fact that a **3-4**<sub>2</sub> complex can form, and initial modeling suggested that polymyxin B can also form a 2:1 complex with **3**. Nevertheless, we were able to take

(17) Zhou, X. T.; Forestier, C.; Goff, R. D.; Li, C.; Teyton, L.; Bendelac, A.; Savage, P. B. *Org. Lett.* **2002**, *4*, 1267–1270.

(18) SPECFIT/32 global analysis system.

(19) Moore, R.; Bates, N. C.; Hancock, R. E. W. *Antimicrob. Agents Chemother.* **1986**, *29*, 496–500.

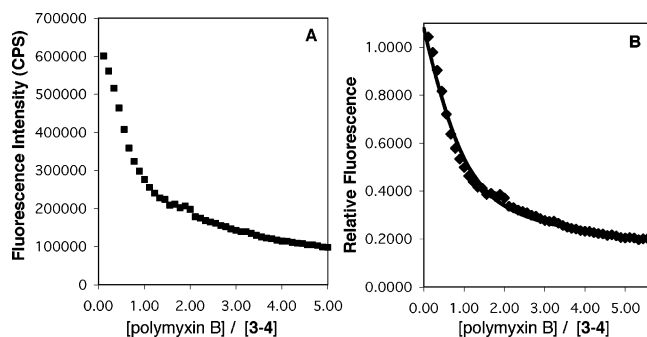


**Figure 5.** (A) Fluorescence intensities ( $\lambda_{\text{em}} = 488 \text{ nm}$ ) from a titration of **3–4** with polymyxin B. Titration was done in aqueous phosphate buffer (5 mM) at pH 7.2. The initial concentration of **3–4** was  $4.1 \mu\text{M}$ . (B) (◆) Titration data with relative fluorescence values; (solid line) calculated values for the competitive titrations using eq 4.

advantage of modeling of similar systems<sup>20</sup> to generate association constants for the interactions of polymyxin B with **3**. The fluorescence of the system,  $F_{\text{tot}}$ , can be represented by the difference of  $F_1$ , which is related to the concentrations of **3–4** and **3–4**<sub>2</sub>, and  $F_2$ , which represents a loss of fluorescence based on formation of **3–polymyxin B** and **3–(polymyxin B)**<sub>2</sub> (eqs 3–5). Equilibrium constants  $K_3$  and  $K_4$  correspond to formation of **3–polymyxin B** and **3–(polymyxin B)**<sub>2</sub> complexes, respectively. Concentrations of **4** and polymyxin B are determined using eqs 6 and 7.

$$F_{\text{obs}} = F_1 - F_2 \quad (3)$$

$$F_1 = \frac{1 + F_{3-4}K_1[\mathbf{4}] + F_{3-4_2}K_1K_2[\mathbf{4}]^2}{1 + K_1[\mathbf{4}] + K_1K_2[\mathbf{4}]^2} \quad (4)$$

$$F_2 = \frac{1 + F_{3-\text{PMB}}K_3[\text{PMB}] + F_{3-\text{PMB}_2}K_3K_4[\text{PMB}]^2}{1 + K_3[\text{PMB}] + K_3K_4[\text{PMB}]^2} \quad (5)$$

PMB = polymyxin B

$$[\mathbf{4}]_{\text{tot}} = [\mathbf{4}] + \frac{[\mathbf{3}]_{\text{tot}}(K_1[\mathbf{4}] + 2K_1K_2[\mathbf{4}]^2)}{1 + K_1[\mathbf{4}] + K_1K_2[\mathbf{4}]^2} \quad (6)$$

$$[\text{PMB}]_{\text{tot}} = [\text{PMB}] + \frac{[\mathbf{3}]_{\text{tot}}(K_3[\text{PMB}] + 2K_3K_4[\text{PMB}]^2)}{1 + K_3[\text{PMB}] + K_3K_4[\text{PMB}]^2} \quad (7)$$

In modeling the reaction, eq 3 was solved iteratively, minimizing the sum of squared errors. The calculated results are compared to measured titration data in Figure 5B. The calculated binding constant for the 1:1 complex formation of **3** with polymyxin B is  $(1.00 \pm 0.26) \times 10^6 \text{ M}^{-1}$ , with the 1:2 binding constant being  $(8.9 \pm 2.3) \times 10^3 \text{ M}^{-1}$  (**3**:polymyxin B). The fact that a 1:2 complex forms is consistent with the stoichiometry measured in our earlier studies of polymyxin B interactions with **3**,<sup>12d</sup> considering that both the 1:1 and 1:2 binding constants contributed to the observed interactions.

Overall, **4** has a higher affinity for **3** than does polymyxin B, and this higher affinity may be the cause of the greater activities of examples of steroid antibiotics, as compared to polymyxin B, against some strains of Gram-negative bacteria<sup>6c</sup> and the greater outer-membrane-permeabilizing capacities of steroid antibiotics as compared to polymyxin B nonapeptide.<sup>6c,d</sup>

Association of polymyxin B with lipid A involves a combination of ionic and hydrophobic interactions,<sup>10–12</sup> with ionic interactions believed to dominate association. It has been proposed that appropriate spacing among cationic groups translates into affinity for lipid A.<sup>10,21</sup> And while cationic steroid antibiotics were originally designed to reproduce the spacing of amine groups in a possible active conformation of polymyxin B,<sup>5a</sup> the higher affinity of **4** for **3** may be a consequence of the relative rigidity of the steroid nucleus in **4**, which may provide a greater degree of preorganization, as compared to the more flexible peptide backbone of polymyxin B.

Considering the potential clinical use of antibiotics such as **4**, the following question arises: Does the relatively high affinity of **4** for lipid A derivative **3** translate into cell selectivity (prokaryote vs eukaryote and Gram-negative vs Gram-positive bacteria)? Comparison of the MIC and MHC values of membrane-active antibiotics only gives an indirect measure of cell selectivity, and we anticipated that **5** would prove useful in directly observing interactions of steroid antibiotics with various cell types. As **5** associates with a bacterial membrane, the environment of the fluorophore is expected to be altered dramatically, especially if it were to insert partially into the membrane. We observed the fluorescence behavior of **5** in the presence of varying concentrations of Gram-negative (*Escherichia coli* (ATCC 25922)) and Gram-positive (*Staphylococcus aureus* (ATCC 25923)) bacteria and eukaryotic cells (Chinese hamster ovary (CHO)). Concentrations of bacterial cells are given in colony-forming units (CFUs); CHO cells can be counted directly. To verify that interactions of **5** were occurring with intact bacteria, cells were repeatedly washed, and the number of CFUs were determined after washing by plating bacterial suspensions on nutrient agar and counting colonies after 24 h of incubation.

The  $\lambda_{\text{em}}$  for **5** ( $1.2 \mu\text{M}$ ) alone in phosphate-buffered saline is 532 nm. This concentration of **5** is well below its MIC values with *E. coli* and *S. aureus*. In the presence of *E. coli* ( $2 \times 10^3$  CFUs/mL), the  $\lambda_{\text{em}}$  shifts to 448 nm and a large increase in fluorescent intensity is observed (Figure 6). The wavelength shift and intensity increase are consistent with the fluorophore moving from a polar into a less polar environment. At this concentration of bacteria, only a relatively small fluorescent background is observed. In the presence of an equivalent number of CFUs of *S. aureus* per milliliter no significant change in the fluorescence of **5** is observed (the fluorescence spectrum of **5** in the presence of  $2 \times 10^4$  CFUs of *S. aureus*/mL is shown in Figure 6). Likewise, the fluorescence of **5** does not appreciably change in the presence of comparable concentrations of CHO cells.

To verify that **5** selectively associates with *E. coli* in the presence of greater numbers of Gram-positive bacteria and CHO cells, the fluorescence response of this antibiotic was measured in a mixture of *E. coli* ( $2.0 \times 10^3$  CFUs), *S. aureus* ( $2.0 \times 10^4$

(20) (a) Eftink, M. R. Fluorescent Methods for Studying Equilibrium Macromolecule-Ligand Interactions. In *Methods in Enzymology*; Brand, L., Johnson, M. L., Eds.; Academic Press: New York, 1997; Vol. 278. (b) Jin, T. J. *Inclusion Phenom. Macrocyclic Chem.* **2003**, *45*, 195–201. (c) Izatt, R. M.; Eatough, D.; Christensen, J. J.; Snow, R. L. *J. Phys. Chem.* **1968**, *72*, 1208–1219.

(21) David, S.; Pérez, L.; Infante, M. R. *Bioorg. Med. Chem. Lett.* **2002**, *12*, 357–360.

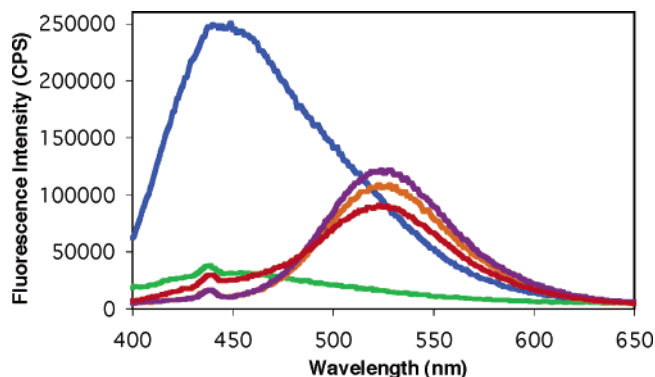


**Figure 6.** Fluorescence spectra of **5** ( $1.2 \mu\text{M}$ ) in phosphate-buffered saline: orange, **5** alone; blue, **5** with  $2.0 \times 10^3$  CFUs of *E. coli*/mL; violet, **5** with  $2.0 \times 10^4$  CFUs of *S. aureus*/mL; red, **5** with  $5.0 \times 10^4$  CHO cells/mL; green, background fluorescence of  $2.0 \times 10^3$  CFUs of *E. coli*/mL.

CFUs), and CHO cells ( $5 \times 10^4$  cells). The fluorescence spectrum of **5** was nearly identical to that measured in the presence of *E. coli* alone, the only difference being a small increase in fluorescence intensity attributable to background fluorescence of the additional cells.

The fluorescent response of **5** to *E. coli* was determined as a function of the number of CFUs per milliliter to find at what bacterial populations **5** is fully bound to the bacterial membrane and a lower detection limit for Gram-negative bacteria. Compound **5** experiences large increases in fluorescence intensity at 448 nm as bacterial populations move from 0 to 500 CFUs/mL, followed by only modest increases in fluorescence as bacterial populations increase (results from a representative titration are shown in Figure 7A). This result suggests that **5** is nearly fully associated with membranes at bacterial populations  $>500$  CFUs/mL, and the response to populations as low as 100 CFUs of *E. coli*/mL can readily be observed. A single cell of *E. coli* is estimated<sup>22</sup> to have a mass of  $10^{-12}$  g, and 100 cells in 1 mL of water constitutes approximately one ten-billionth of the mass of the mixture. Means of rapidly detecting Gram-negative bacteria have been reported,<sup>23</sup> and detection limits above  $10^3$  CFUs/mL were observed.<sup>23,24</sup> The response of **5** to such low numbers of *E. coli* may make it well suited for use in sensing the presence of Gram-negative bacteria especially when selectivity over Gram-positive bacteria is considered (vide infra).

To determine the extent to which **5** interacts preferentially with Gram-negative bacteria, titrations were performed to observe the fluorescent response of **5** to high populations of *S. aureus*. Up to bacterial populations of  $10^6$  CFUs/mL no significant change in the fluorescence of **5** was observed. Above this population, a  $\lambda_{\text{em}}$  shift and intensity increase similar to that observed with 500 CFUs of *E. coli*/mL were observed (Figure 7B). A similar titration was performed with CHO cells, and counts of nearly  $10^6$  cells/mL were also required for a response comparable to 500 CFUs of *E. coli*/mL with the  $\lambda_{\text{em}}$  at 476 nm (Figure 7B).

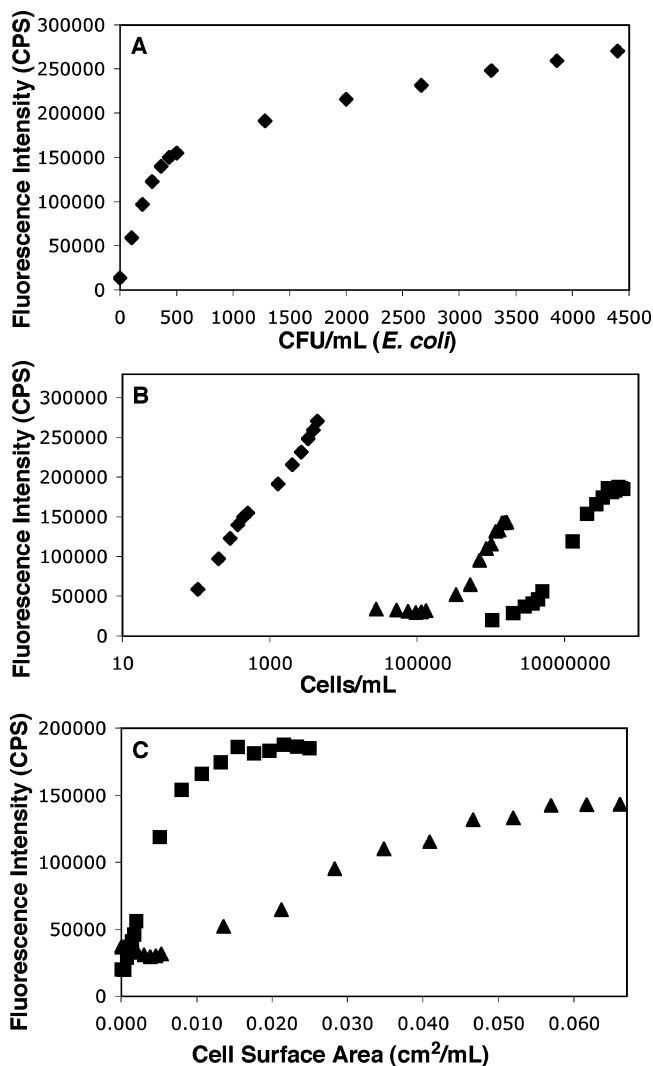


**Figure 7.** (A) Fluorescence intensity (448 nm) of **5** ( $1.2 \mu\text{M}$  in phosphate-buffered saline) upon titration with *E. coli*. (B) Fluorescence intensity of **5** ( $1.2 \mu\text{M}$  in phosphate-buffered saline) upon titration with ( $\blacklozenge$ ) *E. coli* (448 nm), ( $\blacksquare$ ) *S. aureus* (453 nm), and ( $\blacktriangle$ ) CHO cells (476 nm). (C) Fluorescence intensity of **5** ( $1.2 \mu\text{M}$  in phosphate-buffered saline) upon titration with ( $\blacksquare$ ) *S. aureus* (453 nm) and ( $\blacktriangle$ ) CHO cells (476 nm). Cell surface areas were calculated on the basis of reported cell sizes.

It should be noted that comparisons of cell concentrations between CHO cells and bacteria do not take into account the significant size difference between these cell types. The surface area of CHO cells is approximately 75 times larger than that of *E. coli* and more than 100 times larger than that of *S. aureus*.<sup>25</sup> To effectively compare the membrane surface areas presented by *S. aureus* as compared to the much larger CHO cells, fluorescence intensity increases are plotted vs cell surface area (per milliliter) in Figure 7C. Although not as dramatic as the association of **5** with *E. coli*, this antibiotic demonstrates marked selectivity for *S. aureus* over CHO cells. This selectivity may derive from the greater anionic character of the membranes of Gram-positive bacteria as compared to eukaryotic cells.<sup>26</sup>

(22) *Escherichia coli* and *Salmonella typhimurium*. In *Cellular and Molecular Biology*; Neidhardt, F. C., Curtiss, R., Eds.; ASM Press: Washington, DC, 1996; Vol. 1.

(23) (a) Ma, Z.; Li, J.; Jiang, L.; Cao, J.; Bouillanger, P. *Langmuir* **2000**, *16*, 7801–7804. (b) Chan, S.; Horner, S. R.; Fauchet, P. M.; Miller, B. J. *J. Am. Chem. Soc.* **2001**, *123*, 11797–11798.

(24) Detection limits in units of CFUs were not reported in ref 23b. However, using the optical density measurements given and the dilution scheme, CFU limits were well above  $10^3$ /mL.

(25) Cell surface areas are estimated to be (*E. coli*)  $6 \times 10^{-12}$  m<sup>2</sup> (ref 21), (*S. aureus*)  $3 \times 10^{-12}$  m<sup>2</sup> (*Molecular Biology of the Staphylococci*; Novick, R. P., Skurray, R. A., Eds.; VCH Publishers: New York, 1990), and (CHO cells)  $470 \times 10^{-12}$  m<sup>2</sup> (Golzio, M.; Mora, M.-P.; Ruynaud, C.; Delteil, C.; Teissie, J.; Rols, M.-P. *Biophys. J.* **1998**, *74*, 3015–3022).

(26) Mozsolits, H.; Wirth, H.-J.; Werkmeister, J.; Aguilar, M.-I. *Biochim. Biophys. Acta* **2001**, *1512*, 64–76.

## Summary

Direct measurements of interactions of **5** with various cell types suggest that this cationic steroid antibiotic preferentially associates with *E. coli* over *S. aureus* by a factor of over 10000. Taking into account the larger surface area of CHO cells, these data suggest that **5** displays affinity for *E. coli* that is approximately 100000 times greater than that for CHO cells. Of the organisms used in these studies, only *E. coli* presents lipid A in its membranes. We have demonstrated that cationic steroid antibiotic **4** associates with a lipid A derivative with relatively high affinity. We propose that the cell selectivity of cationic steroid antibiotics is directly related to the affinity of these compounds for lipid A, which in turn positively influences their antibacterial activities against Gram-negative bacteria. It is anticipated that further generations of cationic steroid antibiotics with higher affinity for lipid A will display greater antibacterial activity and greater cell selectivity.

## Experimental Section

**Materials and General Methods.**  $^1\text{H}$  NMR and  $^{13}\text{C}$  NMR were recorded on Varian Unity 500 MHz and Varian Unity 300 MHz instruments. Mass spectrometric data were obtained on a JEOL SX 102 A spectrometer. All solvents were dried using activated alumina columns. Chemicals were obtained from Sigma and Aldrich and were used as received unless otherwise noted. All fluorescence measurements were performed with a Jobin Yvon Horiba FluoroMax-3 spectrofluorometer equipped with a Hamilton autotitration injector, F-3005/6.

**Preparation of 7.** Dansyl chloride (21 mg, 0.078 mmol) was added to a solution of **6** (59 mg, 0.064 mmol) and triethylamine (18  $\mu\text{L}$ ) in  $\text{CH}_2\text{Cl}_2$  (5 mL). The mixture was stirred at ambient temperature overnight, and solvent was removed under reduced pressure. After flash column chromatography, **7** (67 mg, 91%) was obtained as a green powder: NMR ( $^1\text{H}$ ,  $\text{CDCl}_3$ )  $\delta$  0.59 (s, 3 H), 0.74 (d,  $J = 5.5$  Hz, 3 H), 0.83–1.06 (m, 8 H), 1.19–1.33 (m, 10 H), 1.43 (s, 27 H), 1.70–1.77 (m, 16 H), 2.05–2.18 (m, 3 H), 2.88 (s, 6 H), 3.06–3.32 (m, 11 H), 3.41–3.69 (m, 8 H), 4.96–5.13 (m, 3 H), 7.18 (d,  $J = 7.32$  Hz, 1 H), 7.49–7.57 (m, 2 H), 8.14 (d,  $J = 7.31$  Hz, 1 H), 8.22 (d,  $J = 8.31$  Hz, 1 H), 8.52 (d,  $J = 8.30$  Hz, 1 H); NMR ( $^{13}\text{C}$ ,  $\text{CDCl}_3$ )  $\delta$  12.35, 14.09, 17.73, 22.42, 22.65, 22.82, 23.25, 24.74, 27.44, 27.56, 28.42, 28.46, 28.39, 28.71, 29.28, 29.62, 29.65, 29.73, 30.07, 30.58, 30.87, 32.75, 34.81, 35.16, 35.19, 38.31, 38.60, 39.28, 39.63, 41.74, 42.43, 43.81, 45.31, 46.05, 46.40, 47.74, 58.98, 65.63, 65.74, 66.13, 75.62, 78.76, 79.23, 80.43, 115.14, 119.50, 123.09, 128.01, 128.80, 129.07, 130.01, 130.04, 130.10, 135.33, 151.67, 156.01, 156.07, 156.20; HRFAB-MS (thioglycerol + Na matrix)  $m/e$  for  $\text{C}_{63}\text{H}_{105}\text{O}_{12}\text{N}_5\text{SNa}$  ( $[\text{M} + \text{Na}]^+$ ) 1178.7396, calcd 1178.7378.

**Preparation of 4.** Methanesulfonyl chloride (5  $\mu\text{L}$ , 0.064 mmol) in  $\text{CH}_2\text{Cl}_2$  (1 mL) was added dropwise to a solution of **7** (36 mg, 0.032 mmol) and triethylamine (18  $\mu\text{L}$ , 0.13 mmol) in  $\text{CH}_2\text{Cl}_2$  (5 mL) at 0  $^\circ\text{C}$  under  $\text{N}_2$ . The mixture was stirred for 1 h, then it was washed with brine (3  $\times$  5 mL), and the organic phase was dried over  $\text{Na}_2\text{SO}_4$ . The solvent was removed under reduced pressure, and crude product was used in the next step of the reaction without further purification. A mixture of the mesylated product *N*-Boc-propyl-1,3-diamine (56 mg, 0.32 mmol), a catalytic amount NaI (2 mg), and  $\text{Na}_2\text{CO}_3$  (34 mg, 0.32 mmol) in THF (2 mL) was refluxed for 48 h. Water (10 mL) was added, and the solution was extracted with ethyl acetate (3  $\times$  10 mL) and dried over  $\text{Na}_2\text{SO}_4$ . After flash column chromatography the fully-Boc-protected form of **4** was obtained as a green powder (21 mg, 51%): NMR ( $^1\text{H}$ ,  $\text{CDCl}_3$ )  $\delta$  0.59 (s, 3 H), 0.74 (d,  $J = 5.5$  Hz, 3 H), 0.83–1.06 (m, 4 H), 1.17–1.33 (m, 9 H), 1.43–1.50 (m, 41 H), 1.57–1.76 (m, 20 H), 2.05–2.18 (m, 2 H), 2.49–2.54 (m, 3 H), 2.78 (s, br, 2 H), 2.87 (s, 6 H), 3.06–3.54 (m, 18 H), 4.96–5.13 (m, 4 H), 7.18 (d,  $J = 7.32$  Hz, 1 H), 7.49–7.57 (m, 2 H), 8.14 (d,  $J = 7.31$  Hz, 1 H), 8.22

(d,  $J = 8.31$  Hz, 1 H), 8.52 (d,  $J = 8.30$  Hz, 1 H); NMR ( $^{13}\text{C}$ ,  $\text{CDCl}_3$ )  $\delta$  12.41, 17.73, 22.43, 22.83, 23.45, 25.06, 27.45, 27.57, 28.13, 28.37, 28.39, 28.42, 28.47, 28.50, 28.71, 29.48, 29.65, 30.06, 30.56, 32.81, 34.82, 35.15, 35.35, 38.32, 38.59, 38.73, 39.34, 39.63, 41.74, 42.44, 44.70, 45.39, 46.08, 46.61, 46.83, 47.26, 65.70, 65.73, 66.27, 75.62, 78.70, 79.21, 80.48, 115.09, 119.56, 123.10, 127.97, 129.48, 129.97, 130.09, 130.13, 135.22, 151.64, 156.06, 156.17; HRFAB-MS (thioglycerol + Na matrix)  $m/e$  for  $\text{C}_{71}\text{H}_{121}\text{O}_{13}\text{N}_7\text{SNa}$  ( $[\text{M} + \text{Na}]^+$ ) 1334.8623, calcd 1334.8641. Removal of the Boc protecting groups was achieved by taking the protected form of **4** (20 mg, 0.015 mmol) and adding 4 M HCl in dioxane (2 mL). The mixture was stirred overnight, and the solvent was removed under reduced pressure. The resulting salt was dissolved in water and lyophilized. The desired product **4** (14 mg, 100%) was obtained as a yellow-green powder: NMR ( $^1\text{H}$ ,  $\text{CDCl}_3$ )  $\delta$  0.67 (s, 3 H), 0.83 (d,  $J = 5.5$  Hz, 3 H), 0.90–0.96 (m, 6 H), 1.28–1.43 (m, 14 H), 1.58–2.01 (m, 18 H), 3.01–3.68 (m, 29 H), 4.20–4.22 (q,  $J = 2.44$  Hz, 1 H), 7.91 (q,  $J = 7.93$  Hz, 2 H), 8.10 (d,  $J = 6.1$  Hz, 1 H), 8.34 (d,  $J = 6.71$  Hz, 1 H), 8.73 (d,  $J = 7.93$  Hz, 1 H), 8.80 (d,  $J = 8.55$  Hz, 1 H); NMR ( $^{13}\text{C}$ ,  $\text{CDCl}_3$ )  $\delta$  11.41, 12.93, 14.40, 18.67, 23.24, 23.72, 24.03, 24.35, 24.93, 25.38, 26.19, 26.51, 26.57, 28.53, 28.69, 28.87, 29.19, 29.38, 29.51, 29.55, 30.12, 31.61, 34.04, 35.89, 36.05, 36.37, 36.57, 37.91, 37.96, 38.00, 39.28, 39.48, 40.15, 40.80, 43.02, 43.76, 44.15, 45.91, 46.11, 46.74, 47.44, 47.72, 47.99, 48.49, 48.58, 48.66, 48.75, 48.79, 48.83, 62.16, 66.26, 66.39, 66.71, 67.64, 68.13, 68.86, 69.07, 72.43, 73.55, 77.74, 80.93, 82.24, 120.53, 127.91, 129.04, 129.86, 131.08, 131.15, 132.41, 133.57, 138.02; HRFAB-MS (thioglycerol + Na matrix)  $m/e$  for  $\text{C}_{51}\text{H}_{89}\text{O}_5\text{N}_7\text{SNa}$  ( $[\text{M} + \text{Na}]^+$ ) 934.6540, calcd 934.6544.

**Preparation of 9.** Methanesulfonyl chloride (58.0 mg, 0.51 mmol) in  $\text{CH}_2\text{Cl}_2$  (5 mL) was added dropwise to a solution of **6** (220 mg, 0.25 mmol) and triethylamine (142  $\mu\text{L}$ , 1.1 mmol) in  $\text{CH}_2\text{Cl}_2$  (20 mL) at 0  $^\circ\text{C}$  under  $\text{N}_2$ . The mixture was stirred for 1 h, then it was washed with brine (3  $\times$  10 mL), and the organic phase was dried over  $\text{Na}_2\text{SO}_4$ . Solvent was removed under reduced pressure, and crude product was used directly in the next step of the reaction. A mixture of the mesylate and  $\text{NaN}_3$  (83.0 mg, 1.27 mmol) in DMSO (1 mL) and THF (1 mL) was heated to 90  $^\circ\text{C}$  for 5 h. Water (10 mL) was added, and the resulting solution was extracted with ethyl acetate (3  $\times$  20 mL) and dried over  $\text{Na}_2\text{SO}_4$ . After flash column chromatography (EtOAc/hexane, 1:1) the desired azide (183 mg, 81%) was obtained as a white solid. This azide (75.6 mg, 0.085 mmol) and triphenylphosphine (111 mg, 0.43 mmol) were stirred in a mixture of THF and water (5:1, 2.4 mL). The solution was stirred overnight. After flash column chromatography ( $\text{CH}_2\text{Cl}_2/\text{MeOH}/\text{NH}_3\text{H}_2\text{O}$ , 10:1.5:0.2) **9** (70 mg, 95%) was obtained as a light yellow solid: NMR ( $^1\text{H}$ ,  $\text{CDCl}_3$ )  $\delta$  0.51 (s, 3 H), 0.72 (s, 3 H), 0.79 (d,  $J = 6.4$  Hz, 3 H), 0.81–0.89 (m, 2 H), 1.18–1.40 (m, 36 H), 1.41–1.82 (m, 17 H), 1.84–2.20 (m, 2 H), 2.40–2.58 (m, 2 H), 2.81–3.20 (m, 10 H), 3.25–3.40 (m, 3 H), 3.41–3.56 (m, 2 H), 4.82–5.34 (m, 3 H); ( $^{13}\text{C}$ ,  $\text{CDCl}_3$ )  $\delta$  12.11, 17.67, 22.17, 22.55, 23.02, 27.16, 27.31, 28.16, 28.19, 28.47, 29.82, 30.25, 32.77, 34.53, 34.90, 35.20, 38.02, 38.25, 39.16, 39.39, 41.49, 42.22, 42.34, 45.78, 46.28, 65.40, 66.11, 75.37, 78.24, 78.88, 80.23, 155.75, 155.91; HRFAB-MS (thioglycerol + Na matrix)  $m/e$   $\text{C}_{48}\text{H}_{88}\text{O}_6\text{N}_4\text{Na}$  ( $[\text{M} + \text{Na}]^+$ ) 887.6447, calcd 887.6449.

**Preparation of 5.** Compounds **9** (30 mg, 0.035 mmol) and **10** (8.8 mg, 0.035 mmol) were mixed in  $\text{CH}_2\text{Cl}_2$  (5 mL) for 12 h. The solvent was removed under reduced pressure. After flash column chromatography (hexane/EtOAc, 1:1) tris-Boc-protected **5** (33 mg, 85%) was obtained as a brown solid: NMR ( $^1\text{H}$ ,  $\text{CDCl}_3$ )  $\delta$  0.51 (s, 3 H), 0.72 (s, 3 H), 0.79 (d,  $J = 6.4$  Hz, 3 H), 0.91–0.99 (m, 4 H), 1.15–1.48 (m, 42 H), 1.51–1.81 (m, 16 H), 1.88–1.92 (m, 1 H), 2.15–2.30 (m, 4 H), 2.62 (t,  $J = 6.5$  Hz, 2 H), 3.05–3.15 (m, 10 H), 3.42–3.55 (m, 3 H), 3.57–3.68 (m, 2 H), 4.82–5.40 (m, 3 H), 6.04 (t,  $J = 1.5$  Hz, 1 H), 6.87 (d,  $J = 2.45$  Hz, 1 H), 7.17 (dd,  $J = 9.28, 2.44$  Hz, 1 H), 7.63 (d,  $J = 8.79$  Hz, 1 H), 7.79 (d,  $J = 8.79$  Hz, 1 H), 7.93 (dd,  $J = 8.79, 1.47$  Hz, 1 H), 8.37 (d,  $J = 1.47$  Hz, 1 H); ( $^{13}\text{C}$ ,  $\text{CDCl}_3$ )  $\delta$  12.38, 14.16,

17.91, 22.46, 22.68, 22.87, 23.31, 25.73, 27.49, 27.59, 28.46, 28.49, 28.52, 28.79, 29.31, 29.36, 29.65, 29.69, 30.09, 30.41, 30.55, 30.71, 31.91, 32.72, 32.92, 34.04, 34.86, 35.16, 38.32, 38.63, 39.52, 39.66, 40.09, 40.42, 41.80, 42.52, 46.10, 46.22, 65.65, 65.82, 66.43, 75.67, 76.75, 76.89, 77.12, 78.76, 79.29, 80.57, 105.26, 116.23, 124.42, 125.01, 126.15, 130.09, 130.77, 137.73, 150.25, 156.09, 156.20, 172.33, 198.49; HRFAB-MS (thioglycerol + Na matrix) *m/e* C<sub>64</sub>H<sub>103</sub>O<sub>11</sub>N<sub>5</sub>Na ([M + Na]<sup>+</sup>) 1140.7551, calcd 1140.7552. The Boc groups were removed by treating the protected form of **5** (30 mg, 0.027 mmol) with 4 M HCl in dioxane (1 mL) for 12 h. The solvent was removed under reduced pressure, and the resulting oil was dissolved in water (5 mL). Lyophilization yielded **5** (22 mg, 100%) as a brown powder: NMR (<sup>1</sup>H, CD<sub>3</sub>OD) δ 0.62 (s, 3 H), 0.82 (s, 3 H), 0.90 (d, *J* = 6.4 Hz, 3 H), 1.10–1.42 (m, 12 H), 1.50–1.62 (m, 2 H), 1.64–2.16 (m, 18 H), 2.60 (t, *J* = 6.5 Hz, 2 H), 2.91–3.20 (m, 12 H), 3.21 (s, 3 H), 3.23 (s, 3 H), 3.38–3.41 (m, 1 H), 3.52–3.78 (m, 4 H), 6.95 (d, *J* = 2.45 Hz, 1 H), 7.26 (dd, *J* = 9.28, 2.44 Hz, 1 H), 7.65 (d, *J* = 8.79 Hz, 1 H), 7.86 (t, *J* = 8.79 Hz, 2 H), 8.44 (d, *J* = 1.47 Hz, 1 H); NMR (<sup>13</sup>C, CD<sub>3</sub>OD) δ 15.42, 21.19, 25.82, 26.23, 26.88, 29.25, 31.06, 31.22, 31.39, 31.71, 31.92, 32.09, 33.33, 36.68, 37.56, 38.40, 38.58, 38.88, 39.03, 41.79, 41.86, 43.32, 43.56, 45.54, 45.88, 46.72, 49.51, 49.94, 50.25, 68.72, 68.91, 69.22, 70.65, 80.26, 83.42, 84.83, 122.33, 129.18, 132.49, 133.30, 134.56, 136.27, 136.50, 139.20, 139.44, 157.82, 177.44, 202.62; HRFAB-MS (thioglycerol + Na matrix) *m/e* C<sub>49</sub>H<sub>79</sub>O<sub>5</sub>N<sub>5</sub>Na ([M + Na]<sup>+</sup>) 840.5993, calcd 840.5979.

**Measurement of Association of 3 with 4.** Slit widths of 5 nm for both monochromators were used. The cell was maintained at a constant temperature (25 ± 0.1 °C) using a circulating water bath. All measurements were recorded from 400 to 650 nm with an excitation wavelength of 340 nm, and each experiment was repeated at least two times. A solution of **3** (27 μM) in phosphate buffer (5 mM, pH 7.2) was added to a quartz cuvette containing a solution of **4** (1.8 mL, 5 μM) in the same buffer under constant stirring. For the titration, 50 injections of 20 μL of the solution of **3** were made. Measurements were made 2 min after each injection to allow for equilibration.

**Displacement Assays with 3–4 and Polymyxin B.** The parameters described above were used in the displacement assays, and the titration was carried out in the same buffer system. A solution of polymyxin B (100 μM) was added in 50 injections of 10 μL to a preequilibrated mixture of **3** and **4** (2.2 mL, 4.1 μM).

**Cell Selectivity Experiments. (a) Growth and Washing of Bacterial Cells.** Inocula of either *E. coli* (ATCC 25922) or *S. aureus*

(ATCC 25923) were added to Muller Hinton broth (4 mL), and the suspension was incubated at 37 °C for 24 h with gentle shaking. To ensure that only whole bacteria were present, the broth solution was replaced by isotonic phosphate-buffered saline (PBS) by centrifuging the bacterial suspensions (1000 rpm, 15 min), removing the supernatant, resuspending the bacteria in PBS, vortexing for 20 s, and repeating the procedure two additional times. Bacterial counts were determined by diluting the resulting suspensions several times and plating 10 μL of each dilution on Muller Hinton agar plates. Colonies were counted after incubation (24 h at 37 °C).

**(b) Growth and Washing of CHO Cells.** CHO cells were grown to confluency in Dulbecco's modified Eagle's medium at 37 °C in an atmosphere of 5% CO<sub>2</sub>. Confluency of the CHO cells was determined using a microscope and measuring the percentage of the bottom of the container covered with CHO cells (100% confluency is approximately 8.8 × 10<sup>6</sup> cells adhered to the bottom of a 25 mL culture flask). The growth medium was removed and replaced by 1 mL of a buffered solution of trypsin (0.05%), and the resulting mixture was gently rocked back and forth for 1 min. The supernatant was removed, and another aliquot of buffered trypsin solution (1 mL) was added. The resulting suspension was rocked for 6 min and then pipetted into a sterile microcentrifuge tube. The cells were washed and suspended in PBS as described above.

**(c) Interactions of 5 with E. coli, S. aureus, and CHO Cells.** Compound **5** was dissolved in PBS at a concentration of 1.2 μM. Titrations were carried out using a dilute and a concentrated cell suspension for each cell type. For experiments with *E. coli*, six aliquots (100 μL) of a 2 × 10<sup>5</sup> CFUs/mL suspension were initially added followed by another 10 aliquots (100 μL) of a 2 × 10<sup>4</sup> CFUs/mL suspension. Fluorescence measurements were made 10 min after addition of cells to allow equilibration. The same procedure was followed with *S. aureus* and CHO cells, except that titrants were 2 × 10<sup>7</sup> and 2 × 10<sup>8</sup> CFUs/mL suspensions for *S. aureus* and 5.3 × 10<sup>5</sup> and 5.3 × 10<sup>6</sup> CFUs/mL suspensions for CHO cells.

**Acknowledgment.** We gratefully acknowledge financial support from the National Institutes of Health (NIGMS).

JA046909P